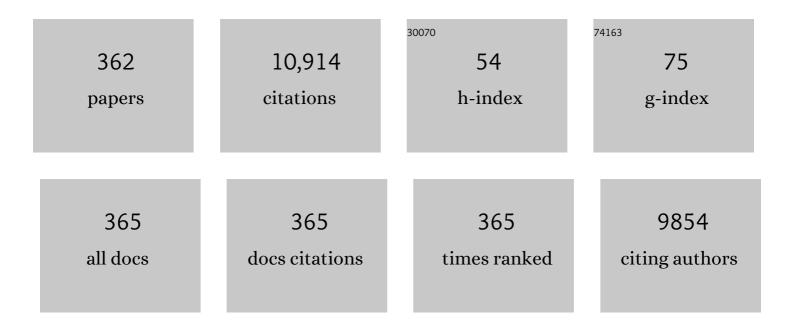
Xun Zhu

List of Publications by Year in descending order

Source: https://exaly.com/author-pdf/179983/publications.pdf Version: 2024-02-01



<u>Хим 7ни</u>

#	Article	IF	CITATIONS
1	Electricity generation and electrochemical insight of zinc-air battery via microfluidic flow control. Chemical Engineering Journal, 2022, 429, 132198.	12.7	6
2	Enhanced gas removal and cell performance of a microfluidic fuel cell by a paper separator embedded in the microchannel. Energy, 2022, 239, 122098.	8.8	10
3	Effects of carbon cloth on anaerobic digestion of high concentration organic wastewater under various mixing conditions. Journal of Hazardous Materials, 2022, 423, 127100.	12.4	49
4	A new heat supply strategy for CO2 capture process based on the heat recovery from turbine exhaust steam in a coal-fired power plant. Energy, 2022, 239, 121817.	8.8	16
5	Hydrothermal hydrolysis of algal biomass for biofuels production: A review. Bioresource Technology, 2022, 344, 126213.	9.6	24
6	Biohydrogen production from microalgae for environmental sustainability. Chemosphere, 2022, 291, 132717.	8.2	81
7	The role of machine learning to boost the bioenergy and biofuels conversion. Bioresource Technology, 2022, 343, 126099.	9.6	76
8	Biomass waste-derived hierarchical porous composite electrodes for high-performance thermally regenerative ammonia-based batteries. Journal of Power Sources, 2022, 517, 230719.	7.8	16
9	Flexible enzymatic biofuel cell based on 1, 4-naphthoquinone/MWCNT-Modified bio-anode and polyvinyl alcohol hydrogel electrolyte. Biosensors and Bioelectronics, 2022, 198, 113833.	10.1	20
10	A flexible on-fiber H2O2 microfluidic fuel cell with high power density. International Journal of Hydrogen Energy, 2022, 47, 4793-4803.	7.1	18
11	ZIF-67-derived Co nanoparticles embedded in N-doped porous carbon composite interconnected by MWCNTs as highly efficient ORR electrocatalysts for a flexible direct formate fuel cell. Chemical Engineering Journal, 2022, 432, 134192.	12.7	39
12	Elimination of Fuel Crossover in a Single-Flow Microfluidic Fuel Cell with a Selective Catalytic Cathode. Industrial & Engineering Chemistry Research, 2022, 61, 1955-1964.	3.7	2
13	A synchronous photoautotrophic-heterotrophic biofilm cultivation mode for Chlorella vulgaris biomass and lipid simultaneous accumulation. Journal of Cleaner Production, 2022, 336, 130453.	9.3	7
14	Revealing the synergistic effects of cells, pigments, and light spectra on light transfer during microalgae growth: A comprehensive light attenuation model. Bioresource Technology, 2022, 348, 126777.	9.6	34
15	Pore-scale modeling of mass transport in the air-breathing cathode of membraneless microfluidic fuel cells. International Journal of Heat and Mass Transfer, 2022, 188, 122590.	4.8	13
16	Synergetic Photo-Thermo Catalytic Hydrogen Production by Carbon Materials. Journal of Physical Chemistry Letters, 2022, 13, 1602-1608.	4.6	12
17	Photothermal trap with multi-scale micro-nano hierarchical structure enhances light absorption and promote photothermal anti-icing/deicing. Chemical Engineering Journal, 2022, 435, 135025.	12.7	58
18	Comparative life cycle and economic assessments of various value-added chemicals' production <i>via</i> electrochemical CO ₂ reduction. Green Chemistry, 2022, 24, 2927-2936.	9.0	7

#	Article	IF	CITATIONS
19	Spontaneous Imbibition in Paper-Based Microfluidic Devices: Experiments and Numerical Simulations. Langmuir, 2022, 38, 2677-2685.	3.5	8
20	How Interfacial Properties Affect Adhesion: An Analysis from the Interactions between Microalgal Cells and Solid Substrates. Langmuir, 2022, 38, 3284-3296.	3.5	10
21	Successful combinatorial therapy of sirolimus and neuraminidase inhibitors in a patient with highly pathogenic avian influenza A (H5N6) virus: a case report. Annals of Translational Medicine, 2022, 10, 265-265.	1.7	1
22	Filter paper membrane based microfluidic fuel cells: Toward next-generation miniaturized and low cost power supply. International Journal of Hydrogen Energy, 2022, 47, 15065-15073.	7.1	11
23	Novel Superaerophobic Anode with Fernâ€Shaped Pd Nanoarray for Highâ€Performance Direct Formic Acid Fuel Cell. Advanced Functional Materials, 2022, 32, .	14.9	18
24	Oxygen self-doping formicary-like electrocatalyst with ultrahigh specific surface area derived from waste pitaya peels for high-yield H2O2 electrosynthesis and efficient electro-Fenton degradation. Separation and Purification Technology, 2022, 289, 120687.	7.9	11
25	Role of defects and oxygen-functional groups in carbon paper cathode for high-performance direct liquid fuel cells. Carbon, 2022, 192, 170-178.	10.3	11
26	How does the electric field make a droplet exhibit the ejection and rebound behaviour on a superhydrophobic surface?. Journal of Fluid Mechanics, 2022, 941, .	3.4	10
27	An environmentally friendly gradient treatment system of copper-containing wastewater by coupling thermally regenerative battery and electrodeposition cell. Separation and Purification Technology, 2022, 295, 121243.	7.9	8
28	Dynamic two-phase flow behaviors in permeable network integrated with microchannel. Applied Thermal Engineering, 2022, , 118639.	6.0	3
29	Lightâ€Fueled Submarine‣ike Droplet. Advanced Science, 2022, 9, .	11.2	7
30	Accelerated bubble growth and departure by bioinspired gradient anode in microfluidic fuel cells. Electrochimica Acta, 2022, 424, 140618.	5.2	10
31	Light Droplet Levitation in Relation to Interface Morphology and Liquid Property. Journal of Physical Chemistry Letters, 2022, 13, 4762-4767.	4.6	3
32	Activated Carbon Facilitates Anaerobic Digestion of Furfural Wastewater: Effect of Direct Interspecies Electron Transfer. ACS Sustainable Chemistry and Engineering, 2022, 10, 8206-8215.	6.7	14
33	Light Controlled 3D Crystal Morphology for Droplet Evaporative Crystallization on Photosensitive Hydrophobic Substrate. Journal of Physical Chemistry Letters, 2022, 13, 5910-5917.	4.6	2
34	Kinetics of light assisted catalytic reduction of 4-NP over Ag/PDA. Chemical Engineering Science, 2022, 259, 117778.	3.8	7
35	Engineering a concordant microenvironment with air-liquid-solid interface to promote electrochemical H2O2 generation and wastewater purification. Separation and Purification Technology, 2022, 297, 121527.	7.9	6
36	Micro-object manipulation by decanol liquid lenses. Lab on A Chip, 2022, 22, 2844-2852.	6.0	5

#	Article	IF	CITATIONS
37	Photothermal reduction of 4-nitrophenol to 4-aminophenol using silver/polydopamine catalysts. Journal of Environmental Chemical Engineering, 2022, 10, 108253.	6.7	4
38	A novel structured foam microreactor with controllable gas and liquid flow paths: Hydrodynamics and nitrobenzene conversion. Chemical Engineering Science, 2021, 229, 116004.	3.8	8
39	Current density distribution in air-breathing microfluidic fuel cells with an array of graphite rod anodes. International Journal of Hydrogen Energy, 2021, 46, 2960-2968.	7.1	16
40	Discrete-holes film fueling anode heads for high performance air-breathing microfluidic fuel cell. Journal of Power Sources, 2021, 482, 228966.	7.8	21
41	Effect of operating parameters on the performance of thermally regenerative ammonia-based battery for low-temperature waste heat recovery. Chinese Journal of Chemical Engineering, 2021, 32, 335-340.	3.5	10
42	In situ visualization of biofilm formation in a microchannel for a microfluidic microbial fuel cell anode. International Journal of Hydrogen Energy, 2021, 46, 14651-14658.	7.1	13
43	Minimizing mass transfer losses in microbial fuel cells: Theories, progresses and prospectives. Renewable and Sustainable Energy Reviews, 2021, 136, 110460.	16.4	28
44	Triple-phase electrocatalysis for the enhanced CO2 reduction to HCOOH on a hydrophobic surface. Chemical Engineering Journal, 2021, 405, 126975.	12.7	56
45	Investigation on effective thermal conductivity of microalgae suspensions in a shear flow. Applied Thermal Engineering, 2021, 186, 116440.	6.0	2
46	How can hydrothermal treatment impact the performance of continuous two-stage fermentation for hydrogen and methane co-generation?. International Journal of Hydrogen Energy, 2021, 46, 14045-14062.	7.1	12
47	Carbon cloth facilitates semi-continuous anaerobic digestion of organic wastewater rich in volatile fatty acids from dark fermentation. Environmental Pollution, 2021, 272, 116030.	7.5	37
48	A high power density paper-based zinc–air battery with a hollow channel structure. Chemical Communications, 2021, 57, 1258-1261.	4.1	12
49	Deep insight into phase transition and crystallization of high temperature molten slag during cooling: A review. Applied Thermal Engineering, 2021, 184, 116260.	6.0	20
50	A 3D oriented CuS/Cu ₂ O/Cu nanowire photocathode. Journal of Materials Chemistry A, 2021, 9, 6971-6980.	10.3	9
51	Route towards high-performance microfluidic fuel cells: a review. Sustainable Energy and Fuels, 2021, 5, 2840-2859.	4.9	16
52	Reduction of Formate Crossover in Sequential-Flow Microfluidic Fuel Cells. Industrial & Engineering Chemistry Research, 2021, 60, 1526-1531.	3.7	3
53	Controllable light-induced droplet evaporative crystallization. Soft Matter, 2021, 17, 8730-8741.	2.7	5
54	Thermoresponsive Surfaces Grafted by Shrinkable Hydrogel Poly(<i>N</i> -isopropylacrylamide) for Controlling Microalgae Cells Adhesion during Biofilm Cultivation. Environmental Science & Technology, 2021, 55, 1178-1189.	10.0	19

#	Article	IF	CITATIONS
55	Performance of a thermally regenerative ammonia-based battery using gradient-porous copper foam electrodes. Science China Technological Sciences, 2021, 64, 696-704.	4.0	6
56	New insights into the role of CO2 in a photocatalytic fuel cell. Journal of Power Sources, 2021, 487, 229438.	7.8	9
57	Hydration Activation of MgO Pellets for CO ₂ Adsorption. Industrial & Engineering Chemistry Research, 2021, 60, 5310-5318.	3.7	5
58	Droplet Evaporation on a Hydrophobic Photothermal Conversion Substrate. Industrial & Engineering Chemistry Research, 2021, 60, 3758-3769.	3.7	14
59	Photothermally Caused Propylene Glycol–Water Binary Droplet Evaporation on a Hydrophobic Surface. Industrial & Engineering Chemistry Research, 2021, 60, 4153-4167.	3.7	3
60	Customizable design strategies for high-performance bioanodes in bioelectrochemical systems. IScience, 2021, 24, 102163.	4.1	20
61	Flipped Quick-Response Code Enables Reliable Blood Grouping. ACS Nano, 2021, 15, 7649-7658.	14.6	12
62	A self-pumping microfluidic fuel cell powered by formate with Pd coated carbon cloth electrodes. Journal of Power Sources, 2021, 490, 229553.	7.8	22
63	Direct Formate/Persulfate Microfluidic Fuel Cell with a Catalyst-Free Cathode and High Power Density. ACS Sustainable Chemistry and Engineering, 2021, 9, 5623-5630.	6.7	10
64	Caregivers: the potential infection resources for the sustaining epidemic of hand, foot, and mouth disease/herpangina in Guangdong, China?. Archives of Public Health, 2021, 79, 54.	2.4	1
65	A fluidized-bed reactor for enhanced mass transfer and increased performance in thermally regenerative batteries for low-grade waste heat recovery. Journal of Power Sources, 2021, 495, 229815.	7.8	10
66	An RFC4/Notch1 signaling feedback loop promotes NSCLC metastasis and stemness. Nature Communications, 2021, 12, 2693.	12.8	38
67	Carbene-Catalyzed Atroposelective Annulation and Desymmetrization of Urazoles. Organic Letters, 2021, 23, 3991-3996.	4.6	50
68	Light-Fueled Beating Coffee-Ring Deposition for Droplet Evaporative Crystallization. Analytical Chemistry, 2021, 93, 8817-8825.	6.5	11
69	Polydopamine inspired dual-functional templates to prepare photoanode with enhanced photoelectrochemical activity. Journal of Power Sources, 2021, 496, 229831.	7.8	7
70	Applying artificial neural network to predict the viscosity of microalgae slurry in hydrothermal hydrolysis process. Energy and AI, 2021, 4, 100053.	10.6	15
71	Infrared laser-induced photothermal phase change for liquid actuation in microchannels. Microfluidics and Nanofluidics, 2021, 25, 1.	2.2	1
72	Kinetics of hydrolysis of microalgae biomass during hydrothermal pretreatment. Biomass and Bioenergy, 2021, 149, 106074.	5.7	10

#	Article	IF	CITATIONS
73	Research status of centrifugal granulation, physical heat recovery and resource utilization of blast furnace slags. Journal of Analytical and Applied Pyrolysis, 2021, 157, 105220.	5.5	36
74	A Novel Stacked Rotary Cup Atomizer Toward Efficient Centrifugal Granulation of Molten Blast Furnace Slag. Steel Research International, 2021, 92, 2100207.	1.8	5
75	Bubble-trap layer for effective removing gas bubbles and stabilizing power generation in direct liquid fuel cell. Journal of Power Sources, 2021, 507, 230260.	7.8	9
76	Self-doped TiO2 nanotube array photoanode for microfluidic all-vanadium photoelectrochemical flow battery. Journal of Electroanalytical Chemistry, 2021, 897, 115598.	3.8	8
77	Carbon-Based Photothermal Superhydrophobic Materials with Hierarchical Structure Enhances the Anti-Icing and Photothermal Deicing Properties. ACS Applied Materials & Interfaces, 2021, 13, 48308-48321.	8.0	102
78	A novel method for carbon removal and valuable metal recovery by incorporating steam into the reduction-roasting process of spent lithium-ion batteries. Waste Management, 2021, 134, 100-109.	7.4	36
79	Boosting photo-biochemical conversion and carbon dioxide bio-fixation of Chlorella vulgaris in an optimized photobioreactor with airfoil-shaped deflectors. Bioresource Technology, 2021, 337, 125355.	9.6	24
80	How can ethanol enhance direct interspecies electron transfer in anaerobic digestion?. Biotechnology Advances, 2021, 52, 107812.	11.7	45
81	Construction of a hierarchical porous surface composite electrode by dynamic hydrogen bubble template electrodeposition for ultrahigh-performance thermally regenerative ammonia-based batteries. Chemical Engineering Journal, 2021, 423, 130339.	12.7	23
82	Solar energy storage by a microfluidic all-vanadium photoelectrochemical flow cell with self-doped TiO2 photoanode. Journal of Energy Storage, 2021, 43, 103228.	8.1	11
83	Life cycle and economic analysis of chemicals production via electrolytic (bi)carbonate and gaseous CO2 conversion. Applied Energy, 2021, 304, 117768.	10.1	15
84	Droplet Migration and Coalescence in a Microchannel Induced by the Photothermal Effect of a Focused Infrared Laser. Industrial & Engineering Chemistry Research, 2021, 60, 1912-1925.	3.7	12
85	Structure design of 3D hierarchical porous anode for high performance microbial fuel cells: From macro-to micro-scale. Journal of Power Sources, 2021, 516, 230687.	7.8	21
86	Domesticating Chlorella vulgaris with gradually increased the concentration of digested piggery wastewater to bio-remove ammonia nitrogen. Algal Research, 2021, 60, 102526.	4.6	22
87	Upper Limit of Light-Levitated Droplet Motion. Analytical Chemistry, 2021, 93, 16008-16016.	6.5	2
88	Light fueled mixing in open surface droplet microfluidics for rapid probe preparation. Physical Chemistry Chemical Physics, 2021, 23, 26356-26365.	2.8	3
89	Loss of ATF4 leads to functional aging-like attrition of adult hematopoietic stem cells. Science Advances, 2021, 7, eabj6877.	10.3	11
90	Superaerophobic hierarchical NiCo-P@Ni electrode for highly efficient hydrogen evolution reaction. The Proceedings of the International Conference on Power Engineering (ICOPE), 2021, 2021.15, 2021-0154.	0.0	0

#	Article	IF	CITATIONS
91	Numerical study of flow and heat transfer characteristics of microalgae slurry in a solar-driven hydrothermal pretreatment system. Applied Thermal Engineering, 2020, 164, 114476.	6.0	10
92	Epidemiological characteristics and phylogenic analysis of human respiratory syncytial virus in patients with respiratory infections during 2011–2016 in southern China. International Journal of Infectious Diseases, 2020, 90, 5-17.	3.3	22
93	Startup cathode potentials determine electron transfer behaviours of biocathodes catalysing CO2 reduction to CH4 in microbial electrosynthesis. Journal of CO2 Utilization, 2020, 35, 169-175.	6.8	54
94	Enhanced current production of the anode modified by microalgae derived nitrogen-rich biocarbon for microbial fuel cells. International Journal of Hydrogen Energy, 2020, 45, 3833-3839.	7.1	17
95	Life cycle and economic assessments of biogas production from microalgae biomass with hydrothermal pretreatment via anaerobic digestion. Renewable Energy, 2020, 151, 70-78.	8.9	43
96	Green and facile synthesis of iron oxide nanoparticle-embedded N-doped biocarbon as an efficient oxygen reduction electrocatalyst for microbial fuel cells. Chemical Engineering Journal, 2020, 385, 123393.	12.7	56
97	Maximum spread of droplets on chemically striped surfaces. AICHE Journal, 2020, 66, e16774.	3.6	6
98	A membraneless microfluidic fuel cell with continuous multistream flow through cotton threads. International Journal of Energy Research, 2020, 44, 2243-2251.	4.5	20
99	Performance of a thermally regenerative ammonia-based flow battery with 3D porous electrodes: Effect of reactor and electrode design. Electrochimica Acta, 2020, 331, 135442.	5.2	27
100	Anion-Exchange Membrane Electrode Assembled Photoelectrochemical Cell with a Visible Light Responsive Photoanode for Simultaneously Treating Wastewater and Generating Electricity. Industrial & Engineering Chemistry Research, 2020, 59, 137-145.	3.7	10
101	Enhancing fuel transport in air-breathing microfluidic fuel cells by immersed fuel micro-jet. Journal of Power Sources, 2020, 445, 227326.	7.8	44
102	Parametric study of biocathodes in microbial electrosynthesis for CO2 reduction to CH4 with a direct electron transfer pathway. Renewable Energy, 2020, 162, 438-446.	8.9	16
103	Solar fuel production from CO2 reduction in a self-biased hybrid solar-microbial device. Applied Energy, 2020, 279, 115821.	10.1	4
104	Biofuel production from wet microalgae biomass: Comparison of physicochemical properties and extraction performance. Energy, 2020, 212, 118581.	8.8	18
105	Fe–N-doped carbon nanoparticles from coal tar soot and its novel application as a high performance air-cathode catalyst for microbial fuel cells. Electrochimica Acta, 2020, 363, 137177.	5.2	10
106	Dynamic behaviors and regime map of a molten blast furnace slag droplet impacting a solid surface. Fuel, 2020, 279, 118451.	6.4	12
107	Performance of a Thermally Regenerative Battery with 3D-Printed Cu/C Composite Electrodes: Effect of Electrode Pore Size. Industrial & amp; Engineering Chemistry Research, 2020, 59, 21286-21293.	3.7	13
108	Modeling for thermal hydrolysis of microalgae slurry in tubular reactor: microalgae cell migration flow and heat transfer effects. Applied Thermal Engineering, 2020, 180, 115784.	6.0	6

#	Article	IF	CITATIONS
109	High performance formic acid fuel cell benefits from Pd–PdO catalyst supported by ordered mesoporous carbon. International Journal of Hydrogen Energy, 2020, 45, 29235-29245.	7.1	31
110	Single-Stream H ₂ O ₂ Membraneless Microfluidic Fuel Cell and Its Application as a Self-Powered Electrochemical Sensor. Industrial & Engineering Chemistry Research, 2020, 59, 15447-15453.	3.7	28
111	CO2 absorption of anhydrous colloidal suspension based silica nanospheres with different microstructures. Energy and Environment, 2020, , 0958305X2094387.	4.6	1
112	3-D printed gradient porous composite electrodes improve anodic current distribution and performance in thermally regenerative flow battery for low-grade waste heat recovery. Journal of Power Sources, 2020, 473, 228525.	7.8	17
113	Antibiotic fidaxomicin is an RdRp inhibitor as a potential new therapeutic agent against Zika virus. BMC Medicine, 2020, 18, 204.	5.5	23
114	Pore-scale modeling of oxygen transport in the catalyst layer of air-breathing cathode in membraneless microfluidic fuel cells. Applied Energy, 2020, 277, 115536.	10.1	23
115	Simultaneous enhancing the sedimentation and adsorption performance of Chlorella vulgaris with montmorillonite modified cationic starch. Biochemical Engineering Journal, 2020, 164, 107785.	3.6	9
116	Preparation of a Catalyst Layer by Layer-by-Layer Self-Assembly for Plate-Type Catalytic Membrane Microreactors. Industrial & Engineering Chemistry Research, 2020, 59, 15865-15874.	3.7	4
117	Simple Method for Directly Synthesizing Ag Nanoparticles with Silver Ammonia and Polydopamine in a Microreactor toward the Conversion of 4-NP to 4-AP. Industrial & Engineering Chemistry Research, 2020, 59, 16205-16216.	3.7	11
118	A direct formate microfluidic fuel cell with cotton thread-based electrodes. International Journal of Hydrogen Energy, 2020, 45, 27665-27674.	7.1	25
119	Light-Caused Droplet Bouncing from a Cavity Trap-Assisted Superhydrophobic Surface. Langmuir, 2020, 36, 11068-11078.	3.5	9
120	Cyclic voltammetry electrodeposition of well-dispersed Pd nanoparticles on carbon paper as a flow-through anode for microfluidic direct formate fuel cells. Nanoscale, 2020, 12, 20270-20278.	5.6	21
121	Neural progenitor cell pyroptosis contributes to Zika virus-induced brain atrophy and represents a therapeutic target. Proceedings of the National Academy of Sciences of the United States of America, 2020, 117, 23869-23878.	7.1	56
122	Effects of Operational Parameters on Biofilm Formation of Mixed Bacteria for Hydrogen Fermentation. Sustainability, 2020, 12, 8863.	3.2	5
123	Pore engineering of graphene aerogels for vanadium redox flow batteries. Chemical Communications, 2020, 56, 14984-14987.	4.1	5
124	Stacked Catalytic Membrane Microreactor for Nitrobenzene Hydrogenation. Industrial & Engineering Chemistry Research, 2020, 59, 9469-9477.	3.7	6
125	Deep neural model with self-training for scientific keyphrase extraction. PLoS ONE, 2020, 15, e0232547.	2.5	12
126	Tumourâ€associated macrophages as a novel target of VEGIâ€251 in cancer therapy. Journal of Cellular and Molecular Medicine, 2020, 24, 7884-7895.	3.6	7

#	Article	IF	CITATIONS
127	Cu/Ni composite electrodes for increased anodic coulombic efficiency and electrode operation time in a thermally regenerative ammonia-based battery for converting low-grade waste heat into electricity. Renewable Energy, 2020, 159, 162-171.	8.9	24
128	Epidemiological characteristics of respiratory viruses in patients with acute respiratory infections during 2009–2018 in southern China. International Journal of Infectious Diseases, 2020, 98, 21-32.	3.3	12
129	C19orf66 interrupts Zika virus replication by inducing lysosomal degradation of viral NS3. PLoS Neglected Tropical Diseases, 2020, 14, e0008083.	3.0	32
130	GO/PEDOT modified biocathodes promoting CO ₂ reduction to CH ₄ in microbial electrosynthesis. Sustainable Energy and Fuels, 2020, 4, 2987-2997.	4.9	37
131	Degradation and transformation of furfural derivatives from hydrothermal pre-treated algae and lignocellulosic biomass during hydrogen fermentation. Renewable and Sustainable Energy Reviews, 2020, 131, 109983.	16.4	21
132	Film fragmentation mode: The most suitable way for centrifugal granulation of large flow rate molten blast slag towards high-efficiency waste heat recovery for industrialization. Applied Energy, 2020, 276, 115454.	10.1	17
133	Dynamic behaviors and charge characteristics of droplet in a vertical electric field before bouncing. Experimental Thermal and Fluid Science, 2020, 119, 110213.	2.7	11
134	Catalytic Membrane Microreactors with an Ultrathin Freestanding Membrane for Nitrobenzene Hydrogenation. ACS Applied Materials & Interfaces, 2020, 12, 9806-9813.	8.0	11
135	Structured Ni–B amorphous alloy catalysts on Ni foam for a gas–liquid–solid microreactor. Catalysis Science and Technology, 2020, 10, 1933-1940.	4.1	2
136	Analysis of the energy barrier between Chlorella vulgaris cells and their interfacial interactions with cationic starch under different pH and ionic strength. Bioresource Technology, 2020, 304, 123012.	9.6	12
137	Hybrid microbial photoelectrochemical system reduces CO2 to CH4 with 1.28% solar energy conversion efficiency. Chemical Engineering Journal, 2020, 390, 124530.	12.7	44
138	<i>In situ</i> formed graphene nanosheets enhance bidirectional electron transfer in bioelectrochemical systems. Sustainable Energy and Fuels, 2020, 4, 2386-2395.	4.9	6
139	Numerical investigation of laminar mixed convection of microalgae slurry flowing in a solar collector. Applied Thermal Engineering, 2020, 175, 115366.	6.0	11
140	Keyphrase Generation With CopyNet and Semantic Web. IEEE Access, 2020, 8, 44202-44210.	4.2	2
141	Sustainable biohythane production from algal bloom biomass through two-stage fermentation: Impacts of the physicochemical characteristics and fermentation performance. International Journal of Hydrogen Energy, 2020, 45, 34461-34472.	7.1	17
142	Predicting the interaction between nanoparticles in shear flow using lattice Boltzmann method and Derjaguin–Landau–Verwey–Overbeek (DLVO) theory. Physics of Fluids, 2020, 32, .	4.0	13
143	Application of bubble carrying to Chlorella vulgaris flocculation with branched cationic starch: An efficient and economical harvesting method for biofuel production. Energy Conversion and Management, 2020, 213, 112833.	9.2	9
144	Pyrolysis kinetics and reaction mechanism of the electrode materials during the spent LiCoO2 batteries recovery process. Journal of Hazardous Materials, 2020, 398, 122955.	12.4	108

#	Article	lF	CITATIONS
145	Photo-bioreactor design for microalgae: A review from the aspect of CO2 transfer and conversion. Bioresource Technology, 2019, 292, 121947.	9.6	86
146	Synergistic effect of Pd content and polyelectrolyte multilayer structure on nitrobenzene hydrogenation in a microreactor. RSC Advances, 2019, 9, 23560-23569.	3.6	4
147	A membrane-less visible-light responsive micro photocatalytic fuel cell with the laterally-arranged CdS/ZnS-TiO2 photoanode and air-breathing CuO photocathode for simultaneous wastewater treatment and electricity generation. Separation and Purification Technology, 2019, 229, 115821.	7.9	23
148	Improved performance of microbial fuel cells using a gradient porous air cathode: An experiment and simulation study. Bioelectrochemistry, 2019, 130, 107335.	4.6	6
149	Reply to Hueston et al. Journal of Infectious Diseases, 2019, 220, 1540-1542.	4.0	0
150	Exergy analyses of biogas production from microalgae biomass via anaerobic digestion. Bioresource Technology, 2019, 289, 121709.	9.6	39
151	Identification of a Novel Betacoronavirus (Merbecovirus) in Amur Hedgehogs from China. Viruses, 2019, 11, 980.	3.3	42
152	A dual-functional three-dimensional herringbone-like electrode for a membraneless microfluidic fuel cell. Journal of Power Sources, 2019, 438, 227058.	7.8	37
153	Simulation on the Marangoni flow and heat transfer in a laser-heated suspended droplet. Chemical Engineering Science, 2019, 209, 115202.	3.8	12
154	Zika Virus Infection Induces Acute Kidney Injury Through Activating NLRP3 Inflammasome Via Suppressing Bcl-2. Frontiers in Immunology, 2019, 10, 1925.	4.8	30
155	Adsorption thermodynamic characteristics of Chlorella vulgaris with organic polymer adsorbent cationic starch: Effect of temperature on adsorption capacity and rate. Bioresource Technology, 2019, 293, 122056.	9.6	28
156	Polarity reversal facilitates the development of biocathodes in microbial electrosynthesis systems for biogas production. International Journal of Hydrogen Energy, 2019, 44, 26226-26236.	7.1	30
157	Visualization of two-phase reacting flow behavior in a gas–liquid–solid microreactor. Reaction Chemistry and Engineering, 2019, 4, 715-723.	3.7	7
158	Rheokinetics of microalgae slurry during hydrothermal pretreatment processes. Bioresource Technology, 2019, 289, 121650.	9.6	13
159	A ternary hybrid CuS/Cu2O/Cu nanowired photocathode for photocatalytic fuel cell. Journal of Power Sources, 2019, 435, 226766.	7.8	22
160	On the centrifugal granulation characteristics by rotary disk: Effect of outer edge structure. Applied Thermal Engineering, 2019, 159, 113977.	6.0	11
161	Long noncoding RNA LINC00673-v4 promotes aggressiveness of lung adenocarcinoma via activating WNT/β-catenin signaling. Proceedings of the National Academy of Sciences of the United States of America, 2019, 116, 14019-14028.	7.1	72
162	Life-cycle assessment of biohythane production via two-stage anaerobic fermentation from microalgae and food waste. Renewable and Sustainable Energy Reviews, 2019, 112, 395-410.	16.4	75

#	Article	IF	CITATIONS
163	Modeling of PEM Fuel Cell Catalyst Layers: Status and Outlook. Electrochemical Energy Reviews, 2019, 2, 428-466.	25.5	60
164	Three-dimensional two-phase simulation of a unitized regenerative fuel cell during mode switching from electrolytic cell to fuel cell. Energy Conversion and Management, 2019, 195, 989-1003.	9.2	37
165	Zika virus antagonizes interferon response in patients and disrupts RIG-l–MAVS interaction through its CARD-TM domains. Cell and Bioscience, 2019, 9, 46.	4.8	42
166	In Situ Synthesis of a Multilayered (PSS-PAH-Pd) _{<i>n</i>} Catalytic Hybrid Film Synthesized by the Layer-by-Layer Self-Assembly. Industrial & Engineering Chemistry Research, 2019, 58, 9038-9047.	3.7	4
167	Core-shell structured Pd catalyst layer encapsulated by polydopamine for a gas-liquid-solid microreactor. Applied Surface Science, 2019, 487, 416-425.	6.1	11
168	Inhibitory effects of furfural and vanillin on two-stage gaseous biofuel fermentation. Fuel, 2019, 252, 350-359.	6.4	10
169	Sea cucumber extract TBLâ€12 inhibits the proliferation, migration, and invasion of human prostate cancer cells through the p38 mitogenâ€activated protein kinase and intrinsic caspase apoptosis pathway. Prostate, 2019, 79, 826-839.	2.3	11
170	Two-phase computational modelling of a membraneless microfluidic fuel cell with a flow-through porous anode. Journal of Power Sources, 2019, 420, 88-98.	7.8	32
171	Lnc <scp>RNA DUXAP</scp> 9â€206 directly binds with Cblâ€b to augment <scp>EGFR</scp> signaling and promotes nonâ€small cell lung cancer progression. Journal of Cellular and Molecular Medicine, 2019, 23, 1852-1864.	3.6	15
172	A solar responsive cubic nanosized CuS/Cu2O/Cu photocathode with enhanced photoelectrochemical activity. Journal of Catalysis, 2019, 372, 182-192.	6.2	28
173	Copper Foam Electrodes for Increased Power Generation in Thermally Regenerative Ammonia-Based Batteries for Low-Grade Waste Heat Recovery. Industrial & Engineering Chemistry Research, 2019, 58, 7408-7415.	3.7	32
174	Improving the electric performance of a unitized regenerative fuel cell during mode switching through mass transfer enhancement. Energy Conversion and Management, 2019, 188, 27-39.	9.2	15
175	Convective heat transfer characteristics of microalgae slurries in a circular tube flow. International Journal of Heat and Mass Transfer, 2019, 137, 823-834.	4.8	12
176	Mass transfer in proton exchange membrane fuel cells with baffled flow channels and a porousâ€blocked baffled flow channel design. International Journal of Energy Research, 2019, 43, 2910-2929.	4.5	41
177	Hierarchical Pd@Ni catalyst with a snow-like nanostructure on Ni foam for nitrobenzene hydrogenation. Applied Catalysis A: General, 2019, 575, 238-245.	4.3	16
178	Effect of geometrical configurations on alkaline air-breathing membraneless microfluidic fuel cells with cylinder anodes. Science China Technological Sciences, 2019, 62, 388-396.	4.0	6
179	A microfluidic all-vanadium photoelectrochemical cell with the N-doped TiO2 photoanode for enhancing the solar energy storage. Journal of Power Sources, 2019, 419, 162-170.	7.8	21
180	Gas consumption characteristics determined by gas-liquid two-phase flow coupled with catalytic reaction in a gas-liquid-solid microreactor. International Journal of Heat and Mass Transfer, 2019, 135, 897-906.	4.8	7

#	Article	IF	CITATIONS
181	Highly Flexible and Ultraprecise Manipulation of Light-Levitated Femtoliter/Picoliter Droplets. Journal of Physical Chemistry Letters, 2019, 10, 1068-1077.	4.6	28
182	MYEOV functions as an amplified competing endogenous RNA in promoting metastasis by activating TGF-β pathway in NSCLC. Oncogene, 2019, 38, 896-912.	5.9	39
183	ECF-induced nuclear localization of SHCBP1 activates β-catenin signaling and promotes cancer progression. Oncogene, 2019, 38, 747-764.	5.9	44
184	pH response of zwitterionic polydopamine layer to palladium deposition in the microchannel. Chemical Engineering Journal, 2019, 356, 282-291.	12.7	10
185	A solar-driven continuous hydrothermal pretreatment system for biomethane production from microalgae biomass. Applied Energy, 2019, 236, 1011-1018.	10.1	55
186	Light-actuated droplets coalescence and ion detection on the CAHTs-assisted superhydrophobic surface. Sensors and Actuators B: Chemical, 2019, 282, 469-481.	7.8	13
187	Biodegradable branched cationic starch with high C/N ratio for Chlorella vulgaris cells concentration: Regulating microalgae flocculation performance by pH. Bioresource Technology, 2019, 276, 133-139.	9.6	48
188	Life-cycle assessment of biofuel production from microalgae via various bioenergy conversion systems. Energy, 2019, 171, 1033-1045.	8.8	114
189	Non-aqueous energy-efficient absorbents for CO2 capture based on porous silica nanospheres impregnated with amine. Energy, 2019, 171, 109-119.	8.8	31
190	Experimental visualization and theoretical analysis of the dynamic impact behavior of a molten blast furnace slag droplet on different surfaces. Applied Thermal Engineering, 2019, 147, 1-9.	6.0	13
191	Heat and mass transfer in a unitized regenerative fuel cell during mode switching. International Journal of Energy Research, 2019, 43, 2678-2693.	4.5	20
192	NLRP3 Inflammasome Activation Mediates Zika Virus–Associated Inflammation. Journal of Infectious Diseases, 2018, 217, 1942-1951.	4.0	69
193	Phase evolution of blast furnace slags with variation in the binary basicity in a variable cooling process. Fuel, 2018, 219, 132-140.	6.4	15
194	Poison tolerance of non-precious catalyst towards oxygen reduction reaction. International Journal of Hydrogen Energy, 2018, 43, 8474-8479.	7.1	21
195	Application of growth-phase based light-feeding strategies to simultaneously enhance Chlorella vulgaris growth and lipid accumulation. Bioresource Technology, 2018, 256, 421-430.	9.6	26
196	Experimental study on the durability of the polydopamine functionalized gas–liquid–solid microreactor for nitrobenzene hydrogenation. RSC Advances, 2018, 8, 5661-5669.	3.6	14
197	Pulsating flow triggered by the laser induced phase change in microchannels with sawtooth-shaped baffles. Sensors and Actuators B: Chemical, 2018, 260, 1018-1024.	7.8	7
198	Investigating the Composition of Iron Salts on the Performance of Microfluidic Fuel Cells. Industrial & & & & & & & & & & & & & & & & & & &	3.7	9

#	Article	IF	CITATIONS
199	Control of the droplet generation by an infrared laser. AIP Advances, 2018, 8, .	1.3	10
200	A ternary hybrid CdS/SiO2/TiO2 photoanode with enhanced photoelectrochemical activity. Renewable Energy, 2018, 127, 524-530.	8.9	27
201	Prediction on crystallization behaviors of blast furnace slag in a phase change cooling process with corrected optical basicity. Fuel, 2018, 223, 360-365.	6.4	9
202	Rheological properties of microalgae slurry for application in hydrothermal pretreatment systems. Bioresource Technology, 2018, 249, 599-604.	9.6	37
203	Granulation characteristics of molten blast furnace slag by hybrid centrifugal-air blast technique. Powder Technology, 2018, 323, 176-185.	4.2	42
204	Interaction of the Taylor flow behaviors and catalytic reaction inside a gas-liquid-solid microreactor under long-term operation. Chemical Engineering Science, 2018, 175, 175-184.	3.8	26
205	Layer-by-layer self-assembly of palladium nanocatalysts with polyelectrolytes grafted on the polydopamine functionalized gas-liquid-solid microreactor. Chemical Engineering Journal, 2018, 332, 174-182.	12.7	26
206	Numerical study on solidification behaviors of a molten slag droplet in the centrifugal granulation and heat recovery system. Applied Thermal Engineering, 2018, 130, 1033-1043.	6.0	31
207	Gas–liquid–solid monolithic microreactor with Pd nanocatalyst coated on polydopamine modified nickel foam for nitrobenzene hydrogenation. Chemical Engineering Journal, 2018, 334, 1897-1904.	12.7	45
208	Physiological-phased kinetic characteristics of microalgae Chlorella vulgaris growth and lipid synthesis considering synergistic effects of light, carbon and nutrients. Bioresource Technology, 2018, 250, 583-590.	9.6	56
209	Boosting Nannochloropsis oculata growth and lipid accumulation in a lab-scale open raceway pond characterized by improved light distributions employing built-in planar waveguide modules. Bioresource Technology, 2018, 249, 880-889.	9.6	42
210	Numerical investigation on phase change cooling and crystallization of a molten blast furnace slag droplet. International Journal of Heat and Mass Transfer, 2018, 118, 471-479.	4.8	24
211	Reduced graphene oxide modified activated carbon for improving power generation of air-cathode microbial fuel cells. Journal of Materials Research, 2018, 33, 1279-1287.	2.6	8
212	Electricity generation of a laminar-flow microbial fuel cell without any additional power supply. RSC Advances, 2018, 8, 33637-33641.	3.6	8
213	A woven thread-based microfluidic fuel cell with graphite rod electrodes. International Journal of Hydrogen Energy, 2018, 43, 22467-22473.	7.1	33
214	A microfluidic all-vanadium photoelectrochemical cell with multi-nanostructured TiO2 photoanode. Journal of Power Sources, 2018, 404, 1-6.	7.8	22
215	Numerical study of water droplets impacting on cylindrical heat transfer pipes. Engineering Applications of Computational Fluid Mechanics, 2018, 12, 598-610.	3.1	5
216	Multilayered Pd nanocatalysts with nano-bulge structure in a microreactor for multiphase catalytic reaction. Chemical Engineering Research and Design, 2018, 138, 190-199.	5.6	8

#	Article	IF	CITATIONS
217	Drag reduction and shear-induced cells migration behavior of microalgae slurry in tube flow. Bioresource Technology, 2018, 270, 38-45.	9.6	8
218	Cassie-to-Wenzel transition of droplet on the superhydrophobic surface caused by light induced evaporation. Applied Thermal Engineering, 2018, 144, 945-959.	6.0	30
219	Optimizing culture conditions for heterotrophic-assisted photoautotrophic biofilm growth of Chlorella vulgaris to simultaneously improve microalgae biomass and lipid productivity. Bioresource Technology, 2018, 270, 80-87.	9.6	41
220	Improving production of volatile fatty acids and hydrogen from microalgae and rice residue: Effects of physicochemical characteristics and mix ratios. Applied Energy, 2018, 230, 1082-1092.	10.1	68
221	Boosting power density of microfluidic biofuel cell with porous three-dimensional graphene@nickel foam as flow-through anode. International Journal of Hydrogen Energy, 2018, 43, 18516-18520.	7.1	12
222	Enhancement of CO2 transfer and microalgae growth by perforated inverted arc trough internals in a flat-plate photobioreactor. Bioresource Technology, 2018, 269, 292-299.	9.6	40
223	Enhancing fermentative hydrogen production with the removal of volatile fatty acids by electrodialysis. Bioresource Technology, 2018, 263, 437-443.	9.6	16
224	IR laser induced phase change behaviors of the NaCl solution in the microchannel. Chemical Engineering Science, 2018, 187, 318-326.	3.8	4
225	Rheological properties of microalgae slurry under subcritical conditions for hydrothermal hydrolysis systems. Algal Research, 2018, 33, 78-83.	4.6	22
226	Hydrothermal hydrolysis pretreatment of microalgae slurries in a continuous reactor under subcritical conditions for large–scale application. Bioresource Technology, 2018, 266, 306-314.	9.6	21
227	A visible-light responsive micro photocatalytic fuel cell with laterally arranged electrodes. Applied Thermal Engineering, 2018, 143, 193-199.	6.0	12
228	Tube-in-tube hollow fiber catalytic membrane microreactor for the hydrogenation of nitrobenzene. Chemical Engineering Journal, 2018, 354, 35-41.	12.7	32
229	Nonsteroidal Anti-inflammatory Drugs Potently Inhibit the Replication of Zika Viruses by Inducing the Degradation of AXL. Journal of Virology, 2018, 92, .	3.4	44
230	A solar responsive photocatalytic fuel cell with the membrane electrode assembly design for simultaneous wastewater treatment and electricity generation. Journal of Hazardous Materials, 2018, 358, 346-354.	12.4	40
231	Centrifugal granulation characteristics of molten blast furnace slag and performance of the granulated particles. Applied Thermal Engineering, 2018, 142, 683-694.	6.0	24
232	Hybrid solar-to-methane conversion system with a Faradaic efficiency of up to 96%. Nano Energy, 2018, 53, 232-239.	16.0	76
233	Novel genetically stable infectious clone for a Zika virus clinical isolate and identification of RNA elements essential for virus production. Virus Research, 2018, 257, 14-24.	2.2	10
234	Epidemiology characteristics of human coronaviruses in patients with respiratory infection symptoms and phylogenetic analysis of HCoV-OC43 during 2010-2015 in Guangzhou. PLoS ONE, 2018, 13, e0191789.	2.5	112

#	Article	IF	CITATIONS
235	Response of anodic biofilm and the performance of microbial fuel cells to different discharging current densities. Bioresource Technology, 2017, 233, 1-6.	9.6	21
236	Optimizing the gas distributor based on CO2 bubble dynamic behaviors to improve microalgal biomass production in an air-lift photo-bioreactor. Bioresource Technology, 2017, 233, 84-91.	9.6	60
237	High-performance optofluidic membrane microreactor with a mesoporous CdS/TiO 2 /SBA-15@carbon paper composite membrane for the CO 2 photoreduction. Chemical Engineering Journal, 2017, 316, 911-918.	12.7	73
238	A simple method for preparing a binder-free paper-based air cathode for microbial fuel cells. Bioresource Technology, 2017, 241, 325-331.	9.6	32
239	A monolithic air cathode derived from bamboo for microbial fuel cells. RSC Advances, 2017, 7, 28469-28475.	3.6	22
240	A self-recirculation electrolyte system for unbuffered microbial fuel cells with an aerated cathode. Bioresource Technology, 2017, 241, 1173-1177.	9.6	6
241	A micro membrane-less photoelectrochemical cell for hydrogen and electricity generation in the presence of methanol. Electrochimica Acta, 2017, 245, 549-560.	5.2	15
242	Simulation on the dynamic flow and heat and mass transfer of a liquid column induced by the IR laser photothermal effect actuated evaporation in a microchannel. International Journal of Heat and Mass Transfer, 2017, 113, 975-983.	4.8	15
243	Startup Performance and Anodic Biofilm Distribution in Continuous-Flow Microbial Fuel Cells with Serpentine Flow Fields: Effects of External Resistance. Industrial & Engineering Chemistry Research, 2017, 56, 3767-3774.	3.7	25
244	Bamboo charcoal as a cost-effective catalyst for an air-cathode of microbial fuel cells. Electrochimica Acta, 2017, 224, 585-592.	5.2	92
245	Uneven biofilm and current distribution in three-dimensional macroporous anodes of bio-electrochemical systems composed of graphite electrode arrays. Bioresource Technology, 2017, 228, 25-30.	9.6	20
246	Astrocyte Elevated Gene 1 Interacts with Acetyltransferase p300 and c-Jun To Promote Tumor Aggressiveness. Molecular and Cellular Biology, 2017, 37, .	2.3	13
247	A membrane electrode assembled photoelectrochemical cell with a solar-responsive cadmium sulfide-zinc sulfide-titanium dioxide/mesoporous silica photoanode. Journal of Power Sources, 2017, 371, 96-105.	7.8	11
248	Step-feed strategy enhances performance of unbuffered air-cathode microbial fuel cells. RSC Advances, 2017, 7, 33961-33966.	3.6	9
249	Phase Change Cooling and Crystallization Characteristics of Blast Furnace Slags with Various MgO/Al ₂ O ₃ Ratios. Energy & Fuels, 2017, 31, 10212-10221.	5.1	13
250	A green, cheap, high-performance carbonaceous catalyst derived from Chlorella pyrenoidosa for oxygen reduction reaction in microbial fuel cells. International Journal of Hydrogen Energy, 2017, 42, 27657-27665.	7.1	45
251	Impact of the accumulation and adhesion of released oxygen during Scenedesmus obliquus photosynthesis on biofilm formation and growth. Bioresource Technology, 2017, 244, 198-205.	9.6	23
252	A microfluidic all-vanadium photoelectrochemical cell for solar energy storage. Electrochimica Acta, 2017, 258, 842-849.	5.2	26

#	Article	IF	CITATIONS
253	Simultaneous enhancement of Chlorella vulgaris growth and lipid accumulation through the synergy effect between light and nitrate in a planar waveguide flat-plate photobioreactor. Bioresource Technology, 2017, 243, 528-538.	9.6	53
254	Cold experiment of slag centrifugal granulation by rotary atomizer: Effect of atomizer configuration. Applied Thermal Engineering, 2017, 111, 1557-1564.	6.0	37
255	An optofluidic planar microreactor for photocatalytic reduction of CO2 in alkaline environment. Energy, 2017, 120, 276-282.	8.8	54
256	Enterovirus 71 Neutralizing Antibodies Seroepidemiological Research among Children in Guangzhou, China between 2014 and 2015: A Cross-Sectional Study. International Journal of Environmental Research and Public Health, 2017, 14, 319.	2.6	10
257	Characteristics of the IR Laser Photothermally Induced Phase Change in Microchannels with Different Depths. Industrial & Engineering Chemistry Research, 2016, 55, 8450-8459.	3.7	7
258	Microfluidic microbial fuel cells: from membrane to membrane free. Journal of Power Sources, 2016, 324, 113-125.	7.8	75
259	Dynamic behaviour of the CO2 bubble in a bubble column bioreactor for microalgal cultivation. Clean Technologies and Environmental Policy, 2016, 18, 2039-2047.	4.1	18
260	Crystallization Behaviors of Blast Furnace (BF) Slag in a Phase-Change Cooling Process. Energy & Fuels, 2016, 30, 3331-3339.	5.1	39
261	Catalytic membrane microreactor with Pd \hat{I}^3 -Al 2 O 3 coated PDMS film modified by dopamine for hydrogenation of nitrobenzene. Chemical Engineering Journal, 2016, 301, 35-41.	12.7	54
262	A novel self-adaptive microalgae photobioreactor using anion exchange membranes for continuous supply of nutrients. Bioresource Technology, 2016, 214, 629-636.	9.6	20
263	Electricity production of a microbial fuel cell stack integrated into a sink drain pipe. Research on Chemical Intermediates, 2016, 42, 7689-7700.	2.7	3
264	Epidemiologic investigation of a family cluster of imported ZIKV cases in Guangdong, China: probable human-to-human transmission. Emerging Microbes and Infections, 2016, 5, 1-7.	6.5	17
265	Comparison of Chlorella vulgaris biomass productivity cultivated in biofilm and suspension from the aspect of light transmission and microalgae affinity to carbon dioxide. Bioresource Technology, 2016, 222, 367-373.	9.6	69
266	High-performance gas-liquid-solid microreactor with polydopamine functionalized surface coated by Pd nanocatalyst for nitrobenzene hydrogenation. Chemical Engineering Journal, 2016, 306, 1017-1025.	12.7	67
267	A three-dimensional nitrogen-doped graphene aerogel-activated carbon composite catalyst that enables low-cost microfluidic microbial fuel cells with superior performance. Journal of Materials Chemistry A, 2016, 4, 15913-15919.	10.3	68
268	An annular photobioreactor with ion-exchange-membrane for non-touch microalgae cultivation with wastewater. Bioresource Technology, 2016, 219, 668-676.	9.6	46
269	Boosting Power Density of Microbial Fuel Cells with 3D Nitrogenâ€Doped Graphene Aerogel Electrode. Advanced Science, 2016, 3, 1600097.	11.2	91
270	Integrating planar waveguides doped with light scattering nanoparticles into a flat-plate photobioreactor to improve light distribution and microalgae growth. Bioresource Technology, 2016, 220, 215-224.	9.6	75

#	Article	IF	CITATIONS
271	Effects of wettability on the growth of Scenedesmus obliquus biofilm attached on glass surface coated with polytetrafluoroethylene emulsion. International Journal of Hydrogen Energy, 2016, 41, 21728-21735.	7.1	30
272	Children's Caregivers and Public Playgrounds: Potential Reservoirs of Infection of Hand-foot-and-mouth Disease. Scientific Reports, 2016, 6, 36375.	3.3	9
273	Optofluidics-Based Membrane Microreactor for Wastewater Treatment by Photocatalytic Ozonation. Industrial & Engineering Chemistry Research, 2016, 55, 8627-8635.	3.7	16
274	A cascading gradient pore microstructured photoanode with enhanced photoelectrochemical and photocatalytic activities. Journal of Catalysis, 2016, 344, 411-419.	6.2	29
275	A micro photocatalytic fuel cell with an air-breathing, membraneless and monolithic design. Science Bulletin, 2016, 61, 1699-1710.	9.0	31
276	Downregulation of VEGF and upregulation of TL1A expression induce HUVEC apoptosis in response to high glucose stimuli. Molecular Medicine Reports, 2016, 13, 3265-3272.	2.4	14
277	Dengue Virus Subverts Host Innate Immunity by Targeting Adaptor Protein MAVS. Journal of Virology, 2016, 90, 7219-7230.	3.4	79
278	SOSTDC1 is down-regulated in non-small cell lung cancer and contributes to cancer cell proliferation. Cell and Bioscience, 2016, 6, 24.	4.8	23
279	A high-sensitivity fiber-optic evanescent wave sensor with a three-layer structure composed of Canada balsam doped with GeO2. Biosensors and Bioelectronics, 2016, 85, 876-882.	10.1	38
280	Improvement on light penetrability and microalgae biomass production by periodically pre-harvesting Chlorella vulgaris cells with culture medium recycling. Bioresource Technology, 2016, 216, 669-676.	9.6	35
281	Midline2 is overexpressed and a prognostic indicator in human breast cancer and promotes breast cancer cell proliferation in vitro and in vivo. Frontiers of Medicine, 2016, 10, 41-51.	3.4	13
282	Optofluidic membrane microreactor for photocatalytic reduction of CO 2. International Journal of Hydrogen Energy, 2016, 41, 2457-2465.	7.1	75
283	IR laser caused droplet evaporation on the hydrophobic surface. International Journal of Heat and Mass Transfer, 2016, 94, 180-190.	4.8	12
284	Effect of CO2 bubbles behaviors on microalgal cells distribution and growth in bubble column photobioreactor. International Journal of Hydrogen Energy, 2016, 41, 4879-4887.	7.1	28
285	Energy–environment–economy evaluations of commercial scale systems for blast furnace slag treatment: Dry slag granulation vs. water quenching. Applied Energy, 2016, 171, 314-324.	10.1	53
286	Influence of the precursor on the porous structure and CO ₂ adsorption characteristics of MgO. RSC Advances, 2016, 6, 19069-19077.	3.6	30
287	Enhancement of microalgae production by embedding hollow light guides to a flat-plate photobioreactor. Bioresource Technology, 2016, 207, 31-38.	9.6	79
288	Crystallization properties of molten blast furnace slag at different cooling rates. Applied Thermal Engineering, 2016, 96, 432-440.	6.0	49

#	Article	IF	CITATIONS
289	Kinetic characteristics and modeling of microalgae Chlorella vulgaris growth and CO2 biofixation considering the coupled effects of light intensity and dissolved inorganic carbon. Bioresource Technology, 2016, 206, 231-238.	9.6	101
290	Enhanced biofilm distribution and cell performance of microfluidic microbial fuel cells with multiple anolyte inlets. Biosensors and Bioelectronics, 2016, 79, 406-410.	10.1	50
291	Lasiodiplodins from mangrove endophytic fungus <i>Lasiodiplodia</i> sp. 318#. Natural Product Research, 2016, 30, 755-760.	1.8	26
292	An investigation of CO2 adsorption kinetics on porous magnesium oxide. Chemical Engineering Journal, 2016, 283, 175-183.	12.7	179
293	Statistical Research on the Bioactivity of New Marine Natural Products Discovered during the 28 Years from 1985 to 2012. Marine Drugs, 2015, 13, 202-221.	4.6	192
294	A New Terminal Cyano Group-containing Benzodiazepine Alkaloid from the Mangrove Endophytic Fungus <i>Penicillium</i> sp. Natural Product Communications, 2015, 10, 1934578X1501000.	0.5	2
295	Biofilm distribution and performance of microfluidic microbial fuel cells with different microchannel geometries. International Journal of Hydrogen Energy, 2015, 40, 11983-11988.	7.1	44
296	Locomotion of bacteria in liquid flow and the boundary layer effect on bacterial attachment. Biochemical and Biophysical Research Communications, 2015, 461, 671-676.	2.1	2
297	Cellular microRNA-miR-548g-3p modulates the replication of dengue virus. Journal of Infection, 2015, 70, 631-640.	3.3	63
298	Analogue experimental study on centrifugal-air blast granulation for molten slag. Applied Thermal Engineering, 2015, 88, 157-164.	6.0	55
299	Centrifugal granulation performance of liquid with various viscosities for heat recovery of blast furnace slag. Applied Thermal Engineering, 2015, 89, 494-504.	6.0	69
300	Experimental and theoretical study on dissolution of a single mixed gas bubble in a microalgae suspension. RSC Advances, 2015, 5, 32615-32625.	3.6	25
301	Solid simultaneous saccharification and fermentation of rice straw for bioethanol production using nitrogen gas stripping. RSC Advances, 2015, 5, 55328-55335.	3.6	14
302	Temperature-independent polymer optical fiber evanescent wave sensor. Scientific Reports, 2015, 5, 11508.	3.3	54
303	Numerical Simulation of Light/Dark Cycle Frequency of Microalgae Fluid in a Helical Tubular Photobioreactor for Carbon Dioxide Capture. International Journal of Green Energy, 2015, 12, 1037-1045.	3.8	4
304	Air-breathing microfluidic fuel cells with a cylinder anode operating in acidic and alkaline media. Electrochimica Acta, 2015, 177, 264-269.	5.2	33
305	Effect of proton transfer on the performance of unbuffered tubular microbial fuel cells in continuous flow mode. International Journal of Hydrogen Energy, 2015, 40, 3953-3960.	7.1	22
306	Computational modeling of alkaline air-breathing microfluidic fuel cells with an array of cylinder anodes. Journal of Power Sources, 2015, 288, 150-159.	7.8	33

#	Article	IF	CITATIONS
307	Lattice Boltzmann simulation on liquid flow and mass transport in a bioreactor with cylinder bundle for hydrogen production. Heat and Mass Transfer, 2015, 51, 859-873.	2.1	5
308	Numerical study on catalytic combustion of methane with ozone using Pd-exchanged zeolite X. Science China Chemistry, 2015, 58, 899-904.	8.2	0
309	Synthesizing MgO with a high specific surface for carbon dioxide adsorption. RSC Advances, 2015, 5, 30929-30935.	3.6	66
310	The Effects of Gas Flow Rate and the Interval Time of Water Supplement on Ethanol Production of Rice Straw by Simultaneous Saccharification and Fermentation. International Journal of Green Energy, 2015, 12, 1031-1036.	3.8	1
311	Performance characteristics of a membraneless solar responsive photocatalytic fuel cell with an air-breathing cathode under different fuels and electrolytes and air conditions. Electrochimica Acta, 2015, 182, 280-288.	5.2	62
312	Respective electrode potential characteristics of photocatalytic fuel cell with visible-light responsive photoanode and air-breathing cathode. International Journal of Hydrogen Energy, 2015, 40, 16547-16555.	7.1	47
313	Aberrantly expressed miR-582-3p maintains lung cancer stem cell-like traits by activating Wnt/β-catenin signalling. Nature Communications, 2015, 6, 8640.	12.8	110
314	Dynamic behaviors of CO2 bubbles coalescing at two parallel capillary orifices in microalgae suspension. International Journal of Heat and Mass Transfer, 2015, 90, 1001-1008.	4.8	20
315	Anolyte recirculation effects in buffered and unbuffered single-chamber air-cathode microbial fuel cells. Bioresource Technology, 2015, 179, 26-34.	9.6	31
316	Increased performance of a tubular microbial fuel cell with a rotating carbon-brush anode. Biosensors and Bioelectronics, 2015, 63, 558-561.	10.1	51
317	IFITM3-containing exosome as a novel mediator for anti-viral response in dengue virus infection. Cellular Microbiology, 2015, 17, 105-118.	2.1	99
318	URGCP promotes non-small cell lung cancer invasiveness by activating the NF-κB-MMP-9 pathway. Oncotarget, 2015, 6, 36489-36504.	1.8	24
319	Estimation of Surface Heat Flux and Surface Temperature during Inverse Heat Conduction under Varying Spray Parameters and Sample Initial Temperature. Scientific World Journal, The, 2014, 2014, 1-13.	2.1	3
320	The Anthraquinone Derivatives from the Fungus Alternaria sp. XZSBG-1 from the Saline Lake in Bange, Tibet, China. Molecules, 2014, 19, 16529-16542.	3.8	15
321	MicroRNA-30e* Suppresses Dengue Virus Replication by Promoting NF-κB–Dependent IFN Production. PLoS Neglected Tropical Diseases, 2014, 8, e3088.	3.0	84
322	Tetravalent recombinant dengue virus-like particles as potential vaccine candidates: immunological properties. BMC Microbiology, 2014, 14, 233.	3.3	25
323	A novel photobioreactor generating the light/dark cycle to improve microalgae cultivation. Bioresource Technology, 2014, 161, 186-191.	9.6	101
324	Metastatic Heterogeneity of Breast Cancer Cells Is Associated with Expression of a Heterogeneous TGFβ-Activating miR424–503 Gene Cluster. Cancer Research, 2014, 74, 6107-6118.	0.9	39

#	Article	IF	CITATIONS
325	Optofluidics based micro-photocatalytic fuel cell for efficient wastewater treatment and electricity generation. Lab on A Chip, 2014, 14, 3368.	6.0	80
326	Meroterpenes and azaphilones from marine mangrove endophytic fungus Penicillium 303#. Fìtoterapìâ, 2014, 97, 241-246.	2.2	48
327	DEPDC1B enhances migration and invasion of non-small cell lung cancer cells via activating Wnt/β-catenin signaling. Biochemical and Biophysical Research Communications, 2014, 450, 899-905.	2.1	55
328	Tubular bamboo charcoal for anode in microbial fuel cells. Journal of Power Sources, 2014, 272, 277-282.	7.8	90
329	High surface area optofluidic microreactor for redox mediated photocatalytic water splitting. International Journal of Hydrogen Energy, 2014, 39, 19270-19276.	7.1	32
330	Epidemiology characteristics of respiratory viruses found in children and adults with respiratory tract infections in southern China. International Journal of Infectious Diseases, 2014, 25, 159-164.	3.3	54
331	Air-breathing direct formic acid microfluidic fuel cell with an array ofÂcylinder anodes. Journal of Power Sources, 2014, 247, 346-353.	7.8	75
332	Computational modeling of air-breathing microfluidic fuel cells with flow-over and flow-through anodes. Journal of Power Sources, 2014, 259, 15-24.	7.8	62
333	Optimization of inner diameter of tubular bamboo charcoal anode for a microbial fuel cell. International Journal of Hydrogen Energy, 2014, 39, 19242-19248.	7.1	18
334	Overexpression of MACC1 and Its significance in human Breast Cancer Progression. Cell and Bioscience, 2013, 3, 16.	4.8	69
335	Effects of brush lengths and fiber loadings on the performance of microbial fuel cells using graphite fiber brush anodes. International Journal of Hydrogen Energy, 2013, 38, 15646-15652.	7.1	33
336	Anodic current distribution in a liter-scale microbial fuel cell with electrode arrays. Chemical Engineering Journal, 2013, 223, 623-631.	12.7	41
337	Performance of a microfluidic microbial fuel cell based on graphite electrodes. International Journal of Hydrogen Energy, 2013, 38, 15710-15715.	7.1	60
338	A review of waste heat recovery technologies towards molten slag in steel industry. Applied Energy, 2013, 112, 956-966.	10.1	339
339	Performance of liter-scale microbial fuel cells with electrode arrays: Effect of array pattern. International Journal of Hydrogen Energy, 2013, 38, 15716-15722.	7.1	12
340	Optofluidic Microreactors with TiO ₂ -Coated Fiberglass. ACS Applied Materials & Interfaces, 2013, 5, 12548-12553.	8.0	57
341	Electrodeposition of Pd catalyst layer on graphite rod electrodes for direct formic acid oxidation. Journal of Power Sources, 2012, 214, 277-284.	7.8	70
342	A Marine Anthraquinone SZ-685C Overrides Adriamycin-Resistance in Breast Cancer Cells through Suppressing Akt Signaling. Marine Drugs, 2012, 10, 694-711.	4.6	31

#	Article	IF	CITATIONS
343	Characterization of the start-up behavior and steady-state performance of biotrickling filter removing low concentration toluene waste gas. Science China Technological Sciences, 2012, 55, 1701-1710.	4.0	3
344	Dynamics of bubble formation and detachment from an immersed micro-orifice on a plate. International Journal of Heat and Mass Transfer, 2012, 55, 3205-3213.	4.8	56
345	Enhanced hydrogen production by Rhodopseudomonas palustris CQK 01 with ultra-sonication pretreatment in batch culture. Bioresource Technology, 2011, 102, 8696-8699.	9.6	23
346	A fractal model for determining oxygen effective diffusivity of gas diffusion layer under the dry and wet conditions. International Journal of Heat and Mass Transfer, 2011, 54, 4341-4348.	4.8	42
347	Molecular dynamics simulation of injection of polyethylene fluid in a variable cross-section nano-channel. Science Bulletin, 2011, 56, 1848-1856.	1.7	5
348	Cytotoxic Naphthoâ€ <i>γ</i> â€pyrones from the Mangrove Endophytic Fungus <i>Aspergillus tubingensis</i> (GX1â€5E). Helvetica Chimica Acta, 2011, 94, 1732-1740.	1.6	35
349	Biofilm formation and electricity generation of a microbial fuel cell started up under different external resistances. Journal of Power Sources, 2011, 196, 6029-6035.	7.8	223
350	An MFC capable of regenerating the cathodic electron acceptor under sunlight. Science China Technological Sciences, 2010, 53, 2489-2494.	4.0	3
351	Experimental Studies of Liquid Droplet Coalescence onÂtheÂGradient Surface. Journal of Superconductivity and Novel Magnetism, 2010, 23, 1165-1168.	1.8	11
352	Numerical Simulation on Coalescence Between a Pair of Drops onÂHomogeneous Horizontal Surface with Volume-of-Fluid Method. Journal of Superconductivity and Novel Magnetism, 2010, 23, 1137-1140.	1.8	7
353	Numerical investigation of water droplet dynamics in a low-temperature fuel cell microchannel: Effect of channel geometry. Journal of Power Sources, 2010, 195, 801-812.	7.8	108
354	Effects of microporous layer preparation on the performance of an air-breathing direct methanol fuel cell. , 2009, , .		0
355	Effect of wettability of anode microporous layer on performance and operation duration of passive air-breathing direct methanol fuel cells. Journal of Applied Electrochemistry, 2009, 39, 1771-1778.	2.9	14
356	Persulfate: A self-activated cathodic electron acceptor for microbial fuel cells. Journal of Power Sources, 2009, 194, 269-274.	7.8	65
357	Numerical simulation of emergence of a water droplet from a pore into a microchannel gas stream. Microfluidics and Nanofluidics, 2008, 4, 543-555.	2.2	57
358	Visualization study on the dynamics of CO2 bubbles in anode channels and performance of a DMFC. Journal of Power Sources, 2007, 171, 644-651.	7.8	84
359	Experimental Investigation on Coalescence of Liquid Drops on Homogeneous Surfaces. , 2006, , .		0
360	Liquid droplet movement on horizontal surface with gradient surface energy. Science in China Series D: Earth Sciences, 2006, 49, 733-741.	0.9	25

#	Article	IF	CITATIONS
361	Modelling of a CH4-producing microbial electrosynthesis system for energy recovery and wastewater treatment. Environmental Science: Water Research and Technology, 0, , .	2.4	Ο
362	A hollow structure for flow and bendable paperâ€based zincâ€air battery. International Journal of Energy Research, 0, , .	4.5	1